Rock property measurements and analysis of selected igneous, sedimentary, and metamorphic rocks from world-wide localities

by

Gordon R. Johnson

U.S. Geological Survey

Open-File report 83-736

1983

Abstract

Dry bulk density and grain density measurements were made on 182 samples of igneous, sedimentary, and metamorphic rocks from various world-wide localities. Total porosity values and both water-accessible and helium-accessible porosities were calculated from the density data. Magnetic susceptibility measurements were made on the solid samples and permeability and streaming potentials were concurrently measured on most samples. Dry bulk densities obtained using two methods of volume determination, namely direct measurement and Archimedes' principle, were nearly equivalent for most samples. Grain densities obtained on powdered samples were typically greater than grain densities obtained on solid samples, but differences were usually small. Sedimentary rocks had the highest percentage of occluded porosity per rock volume whereas metamorphic rocks had the highest percentage of occluded porosity per total porosity. There was no apparent direct relationship between permeability and streaming potential for most samples, although there were indications of such a relationship in the rock group consisting of granites, aplites, and syenites. Most rock types or groups of similar rock types of low permeability had, when averaged, comparable levels of streaming potential per unit of permeability. Three calcite samples had negative streaming potentials.

INTRODUCTION

Various petrophysical properties were measured on 182 specimens of igneous, sedimentary, and metamorphic rocks from two collections that were obtained from Ward's Natural Science Establishment, Inc; namely a standard reference collection of 100 important rock types of North America, and a universal collection that contains rocks from both American and world-wide localities. Table 1 is a compilation of density, porosity, magnetic susceptibility, hydraulic conductivity (permeability), and streaming potential data for all specimens. Rock names used herein were supplied with the collections by Ward's Natural Science Establishment, Inc. A manual that contains petrographic descriptions of all rocks in the North American collection is available from Ward's (catalogue no. 45 W7217), but no such manual exists for the universal collection. However, the latter collection may be purchased with a matching set of thin sections if detailed petrographic analysis is desired. Thin sections corresponding to each rock of the North American collection are also available from Ward's.

SAMPLE MEASUREMENT AND TECHNIQUES OF MEASUREMENTS

The rock samples, as received, were hand-sized specimens from which 25.4 x 25.4 mm cylindrical plugs were cut using a diamond core drill. In some cases, where parent samples were too small, the cylinder lengths were, by necessity, less than 25.4 mm. The cylinder ends were faced using diamond tools and the samples were then dried overnight in a vacuum oven.

Density measurements were obtained on the cylinders using techniques described by Johnson, 1979. Briefly, the samples were weighed dry (W_d) to an accuracy of 0.1 mg, and the bulk volumes (V_b) were obtained by calipering the lengths and diameters. The apparent grain volumes of the cylinders (V_a) were determined using helium pycnometry. The samples were next saturated with distilled water and then weighed both in air and submerged but suspended in a water bath (buoyancy method). From these data dry bulk densities, DBD, and DBA, and grain densities, SGH and SGA were calculated as follows:

$$DBD = \frac{W_d}{V_b}, \quad (1)$$

$$SGH = \frac{W_d}{V_a}, \quad (2)$$

$$DBA = \left(\frac{W_d}{W_s - W_{sp}}\right) \rho, \quad (3)$$

$$SGA = \left(\frac{W_d}{W_d - W_{sp}}\right) \rho, \quad (4)$$

where W_s and W_{sp} are respectively the saturated weights in air and suspended in water. ρ is the density of distilled water at room temperature. While DBD is an absolute measurement within experimental error, SGH and SGA should be considered apparent grain densities unless it is known that helium or water filled all rock pores. Samples need not be completely saturated to obtain an accurate measurement of DBA, but saturation must be sufficient so that the sample does not absorb water while being weighed suspended in water.

Absolute grain densities (SGG) were obtained by crushing and grinding pieces of the hand samples to a grain size considered sufficient to eliminate all pores. The powders were then weighed and the true grain volumes were obtained by helium pycnometry. SGG was calculated using equation (2).

Porosities were calculated from the relation between dry bulk density and grain density. Fractional porosity is, by definition, the ratio of pore volume to the bulk volume of a solid material, but if proper substitutions are made from the equations for bulk density and grain density, fractional porosity (ϕ) can be expressed as

$$\phi = \left(\frac{\text{dry bulk density}}{\text{grain density}}\right) \quad (5)$$

Total porosities (TOP) were calculated from DBD and SGG; water-accessible porosities (WAP) were calculated from DBA and SGA; and helium - accessible porosities (HAP) were calculated from DBD and SGH.

Magnetic susceptibilities were measured using a "Bison bridge", [1] an instrument patterned after a design originally described by Mooney (1952). Subsequently, 121 of the samples were remeasured with a USGS-fabricated magnetic susceptibility system. By then many of the samples used in the original measurements were not available. Those reported susceptibilities that were measured with the Bison bridge are asterisked on table 1.

Permeability, the commonly-used expression for hydraulic conductivity, was measured concurrently with streaming potential in a stainless steel flow cell (fig 1). The extreme range of expected permeabilities required the use of differing amounts of driving or pore pressures (P_1, P_2) to force liquid through the samples. Confining pressures (P_c) were maintained at least 690 kPa greater than pore pressures, and pore pressures ranged from a few kPa to over 2000 kPa. A capillary tube of known inside diameter was affixed to the downstream side of the flow cell and flow rates through the samples were determined by calculating the volume of water displaced in the tube per unit time (q). Permeabilities (k_d), in units of darcies, were calculated from the equation

$$k_d = \frac{q\mu\ell}{\Delta PA}, \quad (5)$$

where μ is the viscosity of the pore fluid, P is net pressure difference through the length of the sample in atmospheres, ℓ is the length, and A the cross-sectional area of the sample. For very permeable samples, downstream water was collected in a cup during a fixed time interval and q was determined using volumes derived from weighing the collected water.

Streaming potential measurements were made immediately after measuring permeability using a "closed" system (fig. 2). A 0.001M KCl solution of distilled water was used for all measurements. In all but a few of the most permeable samples P_c was maintained at about 3450 kPa and (P_1 - P_2) was cycled in increments from 0 to about 2200 kPa. P_1 and P_2 were continuously monitored on a strip chart while voltages between E_1 and E_2 were simultaneously recorded. The electrokinetic coupling coefficient ($\Delta E/ \Delta P$) was determined for each sample by performing a linear regression by the method of least squares on discrete data pairs of E and P_1-P_2 at various P_1. For those few samples that had permeabilities of greater than one darcy, streaming potentials were measured using much lower values of P_c, P_1, and P_2.

DENSITY AND POROSITY

According to Manger (1966) bulk volumes obtained from water displacement measurements (equation 3) may be either too large or too small. If, when weighing a saturated sample in air, a residual film of water remains on the sample surfaces, the value for bulk volume will be too great and the DBA will be too small. On porous samples the surface water film tends to vacate the intergranular apices leaving the near-surface pores free of water which results in bulk volume values that are too small and DBA that are too high. This effect is, of course, increased as pore size increases.

1. "Brand names are cited for purposes of complete description and does not constitute endorsement by the U.S. Geological Survey".

If the ratios of DBD to DBA are compared the above effects can be evaluated. Ratios of greater than one indicate excess surface water when weighing saturated samples in air, whereas ratios of less than one indicate depletion of water from near surface pores. For all specimens the DBD/DBA ratios are 1.00 or less. Approximately 100 specimens have DBD/DBA of 0.99, and 25 specimens have DBD/DBA of less than 0.99. A ratio of 0.99 results from a difference between DBD and DBA values of about 0.03 Mg/m^3 which in turn can be caused by either near-surface water depletion or inaccuracies in calipered volume determinations when making DBD measurements. Of the 25 samples having low DBD/DBA, 13 have chipped edges and one was partially dissolved during saturation. These samples are identified with a superscript 1 or 2 preceding the DBD value. The remaining 11 samples (superscript 3 preceding the DBA value) are either porous sandstones, pumice, scoria, or samples having large surface vugs.

High porosity alone does not necessarily mean that water-saturation bulk density values will be anomalously high. Several very porous specimens have DBD ratios of 0.99-1.00 which can be attributed to small pore size or irregular pore shapes such as so-called ink well pores that limit surface depletion of water when weighing samples in air.

Within experimental error SGH for all samples is equal to or greater than SGA, and SGG is equal to or greater than SGH. These relationships are to be expected because helium will enter a smaller diameter pore than water, and reducing a specimen to powder should eliminate most of the very small pores that may be impermeable to helium. For many samples however, these differences are small. Figure 3 shows a plot of SGA against SGG. Most of the sample points fall along a line having a slope of 1 and passing through the origin. On this line SGA = SGG. If SGA and SGG values (table 1) are within 0.030 Mg/m^3 of each other then SGA is considered to be equal to SGG. Figure 3 shows that a few samples, especially 3 low density-high porosity pumices (table 1), have SGA values that are considerably lower than SGG values. If these 3 samples are omitted the calculated means for all SGA values and SGG values are 2.799 Mg/m^3 and 2.841 Mg/m^3 respectively; a difference of only 0.042 Mg/m^3, or more importantly, a significant difference of only 0.012 Mg/m^3.

All of the different density and porosity measurements were made on only 165 of 182 specimens. The remaining specimens were not wettable because they were either very friable or soluble to some degree in water. Table 2 shows the average densities and porosities of the 165 specimens classified by major rock divisions. DBA is slightly higher than DBD for all three rock types. Likewise SGG is higher than SGA. SGH and SGA values are nearly the same except for sedimentary rocks. The relationship (1-WAP/TOP) indicates that in metamorphic rocks the fractional porosity includes a higher percentage of occluded porosity than in either igneous or sedimentary rocks. But apparently sedimentary rocks have a higher percentage of occluded porosity by rock volume than either igneous or metamorphic rocks owing to their typically higher porosities. For example, sample 89, a sandstone from Santa Clara County, Calif., has a TOP of 19.94%, 0.16 of the total porosity is occluded and 3.15% of the bulk rock is occluded porosity. In contrast, sample 141, a quartzite from Ishpeming, Mich., has a TOP of 1.88%, 0.84 of the total porosity is occluded, but only 1.58% of the bulk rock is occluded porosity. The three low density pumice and scoria specimens were purposely omitted from the porosity tabulations in Table 2 because the porosity of these rocks is very much higher than either the average of the igneous rocks or of individual igneous rocks.

MAGNETIC SUSCEPTIBILITY

Table 1 shows that magnetic susceptibilities have considerable variation between the 182 rock specimens. Low values measured on the Bison bridge were suspect because they were near the threshold sensitivity of the instrument and because the instrument was designed for cylindrical samples at least 50 mm in length (all the specimens used in the measurements were 25 mm or less in length). Although a correction factor for length was applied to the measured susceptibilities it is doubtful whether this factor is applicable to weakly magnetic rocks. For these reasons 121 samples were remeasured on a newly-constructed magnetic susceptibility instrument that has higher precision and sensitivity over a wide range of sample sizes. The relationship between the magnetic susceptibilities measured on both instruments is shown in figure 4. A linear regression analysis made on the data pairs yielded the equation

$$K_o = 0.948K_1 - 0.022 \quad (6)$$

where K_1 and K_o are the magnetic susceptibility values obtained from the USGS-developed instrument and the Bison bridge respectively. The relationship between measured magnetic susceptibility values on both instruments is consistent from about 1×10^{-3} S.I. units to the most intense samples measured. Below 1×10^{-3} S.I. units the data points depart from the line of regression until, at less than about 2×10^{-4} S.I. units, the data pairs do not fit the equation at all. Consequently, equation 6 can be used to convert Bison bridge susceptibility values in table 1 to conform to values obtained on the USGS instrument, but only with certainty above 1×10^{-3} S.I. units and perhaps with a fair degree of certainty between 0.15×10^{-3} and 1×10^{-3} S.I. units. Bison bridge values that are less than 1.5×10^{-3} S.I. units are useful only inasmuch as they indicate that these specimens are weakly magnetic.

PERMEABILITY AND STREAMING POTENTIAL

Permeabilities and streaming potentials were measured jointly because permeability affects the measured streaming potential and, in some rocks permeability changes with time (Anderson, 1981). Streaming potential is defined by the equation

$$E_{str} = \frac{P\varepsilon\delta}{4\pi n_o} (\sigma + 2s/a) \quad (7)$$

where P is the differential pore pressure, ε is the dielectric pemittivity of the liquid, δ is the zeta potential, n_o is the liquid viscosity, σ is the electrical conductivity of the liquid, s is the surface conductivity, and a is the radius of the tube or pore. Permeability is interrelated with the latter term (a), but the quantified effects of permeability in streaming potentials in lithified materials is not well known. Ahmad (1964) reported that streaming potential in a water-sand system increases slightly as permeability decreases. However, most investigators, such as Ishido and Mizutani, 1981, make streaming potential measurements using crushed, seived, and cleaned rock materials thereby controlling the permeability as well as the composition of water flowing through the rock.

In this study solid rock cores were used in an effort to evaluate the effects of permeability on streaming potentials. If all values of permeability in table 1 are plotted against all values of streaming potential there is no apparent correlation. Table 3 shows the arithmetic means of permeabilities and streaming potentials of various rock types or rock groups. Igneous rocks are grouped according to general classifications of acidic to basic rocks. Streaming potentials are reported as electrokinetic coupling coefficients ($\Delta E/\Delta P$) as in table 1. Samples greater than 10 μ darcies were excluded in this tabulation because of their nonuniform permeabilities, and because most of the samples of each rock type or group except sandstone are less than 10 μ darcies. If the highly permeable samples were included the average permeabilities of many of the rock types would be unduly biased. Even so, there is considerable deviation from the arithmetic means of both permeability and electrokinetic coupling coefficient for most rock groupings shown in table 3. The purpose of table 3 is to evaluate the $\Delta E/\Delta P$ of different rocks at a particular level of permeability. There appears to be approximately a direct relationship between average permeabilities and average $\Delta E/\Delta P$, but there are also differences that are not wholly related to permeability. For instance, limestone and marble have about the same average permeabilities, but the $\Delta E/\Delta P$ for marble is nearly twice that of limestone. Slate and phyllite have a very low $\Delta E/\Delta P$ owing to both low permeabilities and clay minerals, the latter which tends to increase the conductivity of the pore water and, consequently, suppress the streaming potential. The low average value of $\Delta E/\Delta P$ for sandstones is most likely the result of clay minerals being present in most of the samples. According to Bogoslovsky and Ogilvy (1972) who made streaming potential measurements in a sand-water system, the absolute values of streaming potentials decrease with increasing clay content. Sample number 84, a red sandstone from Potsdam, N.Y., has a high $\Delta E/\Delta P$ value (0.171 mv/kP_a) compared to the other sandstones; if it were not for this sample the arithmetic mean of $\Delta E/\Delta P$ for sandstones would be much lower. The Potsdam sandstone consists of Cambrian sands that have been cemented by secondary quartz around each of the original grains (Buddington, 1934), and thus is probably a typical orthoquartzite containing little or no clay minerals. Differences in $\Delta E/\Delta P$ between intermediate and acidic and basic igneous rocks are probably related in part to differences in permeabilities but also related in part to dissimilar mineralogies and variations of δ and s.

The last column on table 3 is the ratio between the average permeability and the average $\Delta E/\Delta P$ for each rock group. This column therefore represents $\Delta E/\Delta P$ normalized for the effects of permeability. The values in the last column are about the same for most rock types except for sandstone, slate, and quartz monzonite, etc., which are low, and marble, which is high. These values do not suggest that there is a direct linear relation between permeability and streaming potential; more likely, there is a non-linear relation that was evaluated at only one point in this study, and the streaming potential response per unit of permeability in fact decreases with increasing permeability.

There appears to be a direct correlation between permeability and $\Delta E/\Delta P$ for the granitic and other silicic rocks that are averaged on table 3 (figure 5), though there is a fair amount of scatter in the data points. No other group of rocks showed a clear correlation between permeability and $\Delta E/\Delta P$. If the effects of δ and s (equation 7) could be evaluated then perhaps other correlations between $\Delta E/\Delta P$ and permeability could be found.

Permeabilities were not measureable on samples number 93, 99, 163, and 174, (table 1), but all of these samples had measureable streaming potentials. According to equation 7 a differential pore pressure is necessary in order to generate a streaming potential, implying that these samples must have some intrinsic permeability. Likewise, $\Delta E/\Delta P$ values were less than 0.001 mV/kP_a on samples number 21, 47, 72, 75, and 176, and yet these samples all had measureable permeabilities. It cannot be determined if these samples have any intrinsic streaming potential because this level of $\Delta E/\Delta P$ is about equal to the background noise of the system.

According to Dakhnov, 1959, cations in a water-carbonate rock system, are preferentially adsorbed on the pore surfaces making the streaming potential negative. However, there are 27 carbonate rocks listed in table 1, and only three of these have negative $\Delta E/\Delta P$. Experiments by Somasundaran and Agar, 1967, show that depending on the pH of the pore fluid, the streaming potential of calcite may be either positive or negative. At high pH there is an excess of negative ions whereas at low pH there is an excess of positive ions. These ionic species, however produced, will be absorbed on the pore surfaces in amounts proportional to their concentrations in solution. Therefore, at low pH the streaming potential will be positive and at high pH it will be negative.

As carbonate rocks are dissolved both negative and positive ions will be produced. The relative rates of production of these ionic species will determine whether the streaming potential is negative or positive. The experiments of Somasundaran and Agar further showed that the streaming potential in iceland spar was positive at the onset of repeated measurements, but became negative after considerable elapsed time and as the pH increased. In the present study the streaming potential measurements were all made in about the same time frame. Apparently the three carbonate samples that have negative streaming potentials produced an excess of negative ions soon after insertion into the flow cell. This could have been accomplished by relatively rapid dissolution of these three samples or possibly by chemical factors in the rocks which resulted in more negative ions being produced. At present, however, these are only suppositions based on the above discussion of streaming potentials in carbonate rocks.

SUMMARY AND CONCLUSIONS

Dry bulk densities obtained by using either the direct measurement of volume or the buoyancy method to find the volume are usually comparable if the samples are dimensionally-uniform so that accurate measurements can be made, and if they have no large surface pores or vugs. The effects of excess surface water held in the intergranular apices is negligible when weighing saturated samples in air to determine dry bulk densities.

Accurate measurements of grain density are somewhat method dependent, but for most rocks the differences are minor. Grain densities obtained on solid samples by using either the buoyancy method or helium pycnometry are usually slightly lower than true grain density because of occluded pore spaces which have the effect of increasing the apparent grain volume. In some rock types, such as pumice, this effect is significant. However, sedimentary rocks in general have a higher percentage of occluded porosity per rock volume than either igneous or metamorphic rocks, whereas metamorphic rocks have the most occluded porosity per fractional porosity.

Magnetic susceptibility measurements made using a Bison bridge compare favorably with measurements made on a USGS-built instrument. At less than 1×10^{-3} S.I. units, the Bison bridge becomes progressively inaccurate.

Permeability cannot be directly correlated with streaming potential or any other petrophysical property that was measured on the suite of 182 rock samples. However, if samples of less than 10 μdarcies permeability are grouped into various rock types, there seems to be a more or less direct relationship between average permeabilities and average streaming potentials. Most of these rock types have about the same level of streaming potential when normalized per unit of permeability. Exceptions are sandstone, slate, and quartz monzonite-monzonite granodiorite which have less than average streaming potential per unit permeability and marble which has greater than average streaming potential per unit permeability. Slates and most sandstones have suppressed streaming potentials, probably due to clay minerals which have the effect of increasing the conductivity of the pore fluid in these rocks. It is not known why marble has an anomalously-high streaming potential per unit permeability. The foregoing relations, are only approximate owing to the sparse number of samples for most rock types and owing to large standard deviations of average permeabilities and streaming potentials.

Only three carbonate samples had negative streaming potentials. As calcite dissolves, both positive and negative ions are produced in the pore fluid, and the relative amounts of these two ion species near the rock-water interface is thought to affect the polarity of the streaming potential.

ACKNOWLEDGEMENTS

The following U.S. Geological Survey part time technical personnel contributed to the data collection. Jay Sampson and Patrick Moore assisted in the sample preparation, and Patrick Moore made the density measurements and magnetic susceptibility measurements using the Bison bridge. Davin Larson and Pamela Mohr assisted in measuring permeabilities and streaming potentials.

REFERENCES CITED

Ahmad. Moid Uddin, 1964, A laboratory study of streaming potentials: Geophysical Prospecting, v. 12, no. 1, pp. 49-64.

Anderson, Lennart A., 1981, Rock property analysis of core samples from the Yucca Mountain UE25a-1 borehole, Nevada Test Site, Nevada: U.S. Geological Survey Open-File Report 81-1338, 36 p.

Bogoslovsky, V. A., and Ogilvy, A. A., 1972, The study of streaming potentials on fissured media models: Geophysical Prospecting, v. 20, no. 1, pp. 109-117.

Buddington, A. F., 1934, Geology and mineral resources of the Hammond, Antwerp, and Lowville quadrangles: New York State Museum Bulletin, no. 296, 251 p.

Dakhnov, V. N., 1959, Geophysical well logging: Quarterly of the Colorado School of Mines, Translated into English by George V. Keller, v. 57, no. 2, April, 1962, 445 p.

Ishido, Tsuneo, and Mizutani, Hitoshi, 1981, Experimental and theoretical basis of electrokinetic phenomena in rock-water systems and its applications to geophysics: Journal of Geophysical Research, v. 86, no. 133, pp. 1763-1775.

Johnson, G. R., 1979, Textural properties, in Hunt, G.R., Johnson, G. R., Olhoeft, G. R., Watson, D. E., and Watson, K., Initial report of the petrophysics laboratory: U.S. Geological Survey Circular 789, pp. 67-74.

Manger, G., Edward, 1966, Method-dependent values of bulk, grain, and pore volume as related to observed porosity: U.S. Geological Survey Bulletin, 1203-D, 20 p.

Mooney, Harold M., 1953, Magnetic susceptibility measurements in Minnesota: Geophysics, v. 17, no. 3, p. 531-543.

Somasundaran, P., and Agar, G. E., 1967, The zero point of charge of calcite: Journal of colloid and Interface Science, v. 24, p. 433-440.

Table 1 Selected petrophysical measurements of 182 samples of igneous, sedimentary and metamorphic rocks. [DBD, dry bulk density using calipered volume, DBA and SGA, dry bulk density and grain density using bulk and grain volume determined from Achimedes principle (buoyancy method); SGH and SGG, grain density using volume obtained by helium pycnometry on solid and powdered samples respectively; TOP, WAP, HAP, total, water-accessible, and helium-accessible porosity, in per cent; K, magnetic susceptibility (asterisked values measured on Bison bridge) k_d, hydraulic conductivity or permeability; $\Delta E/\Delta P$, electrokinetic coupling coefficient derived from streaming potential measurement; N/M = not measurable; Leader (--) indicates measurement not possible.

Sample Number	Rock Type & Locality	DBD	DBA	SGG	SGH	SGA	TOP	WAP	HAP	K x 10^3	k_d	$\Delta E/\Delta P$
				Mg/m^3			$100\left[1-\frac{DBD}{SGG}\right]$	$100\left[1-\frac{DBA}{SGA}\right]$	$100\left[1-\frac{DBD}{SGH}\right]$	S.I. units	μdarcies	mV/kP_a
1	Biotite granite, Barre, Vermont	2.642	2.645	2.691	2.675	2.666	1.82	0.79	1.23	*0.15	0.75	0.061
2	Muscovite-Biotite granite, Concord, N.H.	2.629	2.628	2.681	2.662	2.654	1.94	0.98	1.24	*0.22	5.44	0.131
3	Biotite-hornblende granite, St. Cloud Minn.	2.689	2.682	2.740	2.710	2.693	1.86	0.41	0.78	*0.55	0.871	0.032
4	Akalic granite, Quincy, Mass.	2.631	2.630	2.707	2.652	2.649	2.81	0.72	0.79	*0.22	1.80	0.039
5	Aplite, Boulder, Colo.	2.582	2.590	2.634	2.621	2.622	1.97	1.22	1.49	*0.27	2.98	0.065
6	Aplite, San Bernadino Co., Calif.	2.588	2.616	2.635	2.635	2.630	1.78	0.53	1.78	4.11	0.259	0.044
7	Biotite granite, Rockport, Mass.	2.582	2.619	2.676	2.654	2.640	3.51	0.80	2.71	4.71	3.52	0.085
8	Pegmatite, Mitchell Co. N. C.	2.595	2.616	2.631	2.630	2.634	1.37	0.68	1.33	0.26	3.99	0.335

Sample Number	Rock Type & Locality	DBD	DBA	SGG	SGH	SGA	TOP	WAP	HAP	K x 10^3	k_d	$\Delta E/\Delta P$
		Mg/m^3					$100\left[1-\frac{DBD}{SGG}\right]$	$100\left[1-\frac{DBA}{SGA}\right]$	$100\left[1-\frac{DBD}{SGH}\right]$	S.I. units	μdarcies	mV/kP_a
9	Quartz monzonite porphyry, Garfield, Colo.	2.724	2.721	2.759	2.740	2.744	1.27	0.84	0.58	30.72	0.737	0.007
10	Quartz monzonite porphyry, San Bernadino Co., Calif.	2.586	2.611	2.654	2.632	2.645	2.56	1.29	1.75	*15.34	1.86	0.005
11	Granodiorite, St. Cloud, Minn.	2.729	2.729	2.747	2.741	2.735	0.66	0.22	0.44	*28.48	0.923	0.015
12	Granodiorite porphyry, Riverside Co., Calif.	2.666	2.661	2.701	2.670	2.675	1.30	0.52	0.15	8.08	0.502	0.006
13	Obsidian, Lake Co., Oreg.	2.351	2.353	2.374	2.357	2.353	0.97	0.00	0.25	---	0.055	0.017
14	Obsidian, Mineral Co., Nev.	2.343	2.351	2.405	2.362	2.352	2.58	0.04	0.80	0.28	0.054	0.023
15	Snowflake obsidian, Millard Co., Utah	2.344	2.340	2.375	2.350	2.340	1.31	0.00	0.26	1.75	0.026	0.006
16	Pumice, Millard Co., Utah	0.652	[3]0.718	2.366	1.734	1.708	72.44	62.40	57.96	*0.23	0.140×10^6	0.132

Sample Number	Rock Type & Locality	DBD	DBA	SGG	SGH	SGA	TOP	WAP	HAP	K x 10^3	k_d	$\Delta E/\Delta P$
				Mg/m^3			$100\left[1-\frac{DBD}{SGG}\right]$	$100\left[1-\frac{DBA}{SGA}\right]$	$100\left[1-\frac{DBD}{SGH}\right]$	S.I. units	μdarcies	mV/kP_a
17	Pumice, Mono Co., Calif.	0.433	[3]0.505	2.357	1.406	1.368	81.63	63.08	69.20	*0.34	$12.2x10^6$	2.23
18	Rhyolite Tuff, Frying Pan Basin, Mont.	1.279	[3]1.308	2.573	2.570	2.480	50.29	47.26	50.23	*0.32	$0.034x10^6$	0.790
19	Rhyolite, Castle Rock, Colo.	1.924	1.921	2.513	2.510	2.490	23.44	22.85	23.35	*0.20	290.0	0.034
20	Rhyolite porphyry, Chaffee Co., Colo.	2.203	2.209	2.632	2.619	2.616	16.30	15.56	15.88	*1.10	163.0	0.068
21	Rhyolite Porphyry, Kern Co., Calif.	2.430	2.437	2.651	2.627	2.629	8.34	7.30	7.50	1.96	0.430	<0.001
22	Hornblende syenite, York Co., Maine	2.661	2.673	2.705	2.696	2.702	1.63	1.07	1.30	15.67	0.786	0.029
23	Alkalic Syenite Cripple Creek, Colo.	2.590	2.594	2.625	2.598	2.613	1.33	0.73	0.31	43.05	0.227	0.031
24	Nepheline syenite, Blue Mtn., Methuen Twp, Ontario	2.580	2.582	2.669	2.604	2.594	3.33	0.46	0.92	*0.47	5.67	0.088
25	Nepheline-sodalite syenite, Red Hill, N.H.	2.596	2.608	2.653	2.642	2.630	2.15	0.84	1.74	*4.85	0.480	0.045
26	Syenite, Magnet Cove, Ark.	2.511	2.508	2.591	2.549	2.567	3.09	2.30	1.49	23.94	3.42	0.069

Sample Number	Rock Type & Locality	DBD	DBA	SGG	SGH	SGA	TOP	WAP	HAP	K x 10^3	k_d	$\Delta E/\Delta P$
				Mg/m^3			$100\left[1-\frac{DBD}{SGG}\right]$	$100\left[1-\frac{DBA}{SGA}\right]$	$100\left[1-\frac{DBD}{SGH}\right]$	S.I. units	μ darcies	mV/kP_a
27	Augite syenite, Larvik, Norway	2.722	2.731	2.769	2.741	2.733	1.70	0.07	0.69	*22.12	0.103	0.006
28	Sodalite syenite, Ice River, B.C.	2.716	2.720	2.740	2.738	2.734	0.88	0.51	0.80	0.87	1.14	0.027
29	Trachyte porphyry (Bostonite), Essex Co., N.Y.	2.554	2.557	2.639	2.579	2.612	3.22	2.11	0.97	0.09	0.035	0.038
30	Trachyte porphyry, Cripple Creek, Colo.	2.432	2.431	2.674	2.670	2.662	9.05	8.68	8.91	*0.31	2.37	0.007
31	Trachyte porphyry, Bannockburn Twp., Ontario	2.641	2.655	2.673	2.662	2.664	1.20	0.34	0.79	*0.26	0.225	0.006
32	Shonkinite, San Bernadino Co., Calif.	2.781	--	2.986	2.984	--	6.87	--	6.80	10.26	4.76	0.008
33	Ijolite, McClure Mtn., Colo.	2.985	2.977	3.051	3.040	3.021	2.16	1.46	1.81	*1.04	0.125	0.014
34	Siderite carbonatite, Iron Hill, Colo.	2.920	2.920	2.941	2.935	2.932	0.71	0.41	0.51	*0.37	3.37	0.058
35	Phonolite, Cripple Creek, Colo.	2.539	2.533	2.603	2.541	2.557	2.46	0.94	0.08	3.90	0.461	0.004

Sample Number	Rock Type & Locality	DBD	DBA	SGG	SGH	SGA	TOP	WAP	HAP	K x 10^3	k_d	$\Delta E/\Delta P$
				Mg/m^3			$100\left[1-\frac{DBD}{SGG}\right]$	$100\left[1-\frac{DBA}{SGA}\right]$	$100\left[1-\frac{DBD}{SGH}\right]$	S.I. units	μ darcies	mV/kP_a
36	Rhomb porphyry Slagen, Tonsberg Norway	2.655	2.660	2.735	2.730	2.732	2.93	2.64	2.75	*0.91	0.349	0.004
37	Quartz Monzonite, Los Angeles, Calif.	2.655	2.656	2.708	2.663	2.671	1.96	0.56	0.30	10.81	0.730	0.004
38	Monzonite, Silverton, Colo.	2.662	2.679	2.717	2.707	2.722	2.02	1.58	1.66	64.30	0.034	0.006
39	Latite porphyry, Bear Paw Mtns., Montana	2.491	2.486	2.664	2.629	2.599	6.49	4.35	5.25	*5.25	0.289	0.002
40	Tonalite, San Diego, Calif.	2.778	2.769	2.804	2.793	2.783	0.93	0.50	0.54	*0.72	0.037	.011
41	Diorite, Los Angeles Co., Calif.	2.885	2.888	2.955	2.934	2.934	2.37	1.57	1.67	*2.88	0.213	0.029
42	Orbicular diorite, Davie Co., N. C.	2.812	2.833	3.033	3.027	3.009	7.29	5.85	7.10	0.40	14.3	0.010
43	Diorite porphyry, Jackson, Wyo.	2.412	2.423	2.727	2.706	2.678	11.55	9.52	10.86	10.75	0.168	0.002
44	Dacite, N.W. of Helena, Mont.	2.478	2.482	2.702	2.668	2.649	8.29	6.30	7.12	51.57	1.55	0.004
45	Hornblende andesite, Mt. Shasta, Calif.	2.430	2.424	2.655	2.497	2.516	8.47	3.66	2.68	*0.47	0.065	0.002

Sample Number	Rock Type & Locality	DBD	DBA	SGG	SGH	SGA	TOP	WAP	HAP	K x 10^3	k_d	$\Delta E/\Delta P$
		Mg/m^3					$100\left[1-\frac{DBD}{SGG}\right]$	$100\left[1-\frac{DBA}{SGA}\right]$	$100\left[1-\frac{DBD}{SGH}\right]$	S.I. units	μ darcies	mV/kP_a
46	Hornblende andesite porphyry, Gallatin Co., Mont.	2.732	2.746	2.809	2.766	2.775	2.74	1.05	1.23	69.62	0.038	0.001
47	Camptonite, Hoover Dam, Ariz.	2.554	2.592	2.871	2.868	2.867	11.04	9.59	10.95	2.57	0.152	<0.001
48	Tridymite Dacite San Diego Co., Calif.	2.146	2.155	2.603	2.592	2.604	17.56	17.24	17.21	6.60	0.296	0.006
49	Hornblende gabbro, San Diego Co., Calif.	2.977	2.985	3.015	2.996	2.987	1.26	0.07	0.63	198.46	0.138	0.054
50	Norite, Wollaston Twp., Ontario	2.868	2.880	2.925	2.893	2.896	1.95	0.55	0.86	*32.87	2.13	0.037
51	Olivine gabbro, Wichita Mtns. Okla.	2.912	2.926	2.939	2.962	2.961	0.92	1.18	1.69	*7.00	10.3	0.009
52	Hornblende gabbro, Salem, Mass.	3.013	3.037	3.028	3.027	3.040	0.50	0.10	0.46	*75.17	0.043	0.005
53	Anorthosite, Elisabethtown, N. Y.	2.719	2.720	2.766	2.735	2.726	1.70	0.22	0.59	*0.27	0.111	0.008
54	Diabase, Jersey City, N. J.	3.066	3.067	3.086	3.084	3.082	0.65	0.49	0.58	3.67	0.167	0.025
55	Scoria, Klamath Falls, Oreg.	2.035	[3]2.162	2.835	2.865	2.829	28.22	23.58	28.97	*1.18	8,280.0	0.156

Sample Number	Rock Type & Locality	DBD	DBA	SGG	SGH	SGA	TOP	WAP	HAP	K x 10^3	k_d	$\Delta E/\Delta P$
		Mg/m^3					$100\left[1-\frac{DBD}{SGG}\right]$	$100\left[1-\frac{DBA}{SGA}\right]$	$100\left[1-\frac{DBD}{SGH}\right]$	S.I. units	μdarcies	mV/kP_a
56	Amydaloidal Basalt, Keweenan County, Mich.	2.764	[3]2.810	3.213	3.118	3.127	13.97	10.14	11.35	*0.70	61.6	0.270
57	Basalt, Chimney Rock, N. J.	2.930	2.933	2.950	2.933	2.953	0.68	0.68	0.10	44.65	0.101	0.005
58	Olivine Basalt Porphyry, Valmont, Colo.	2.820	2.816	2.828	2.812	2.824	0.28	0.28	0.00	82.12	0.201	0.022
59	Diabase Porphyry, Cape Ann, Mass.	2.883	2.890	2.926	2.902	2.905	1.47	0.52	0.65	*1.17	0.037	0.003
60	Syenogabbro, Butte, Mont.	2.820	2.849	2.925	2.898	2.900	3.59	1.76	2.69	20.13	22.2	0.027
61	Gabbro, Duluth, Minn.	2.919	2.940	2.948	2.933	2.945	0.98	0.17	0.48	138.48	0.541	0.033
62	Norite, wollaston twp., Ontario, Canada	2.902	2.901	2.949	2.943	2.934	1.59	1.12	1.39	7.01	0.132	0.002
63	Anorthosite, San Gabriel, Calif.	[1]2.936	2.982	3.029	3.028	3.039	3.07	1.88	3.04	0.08	10.3	0.019
64	Diabsse, St. Peters', Pa.	3.000	3.045	3.078	3.066	3.067	2.53	0.72	2.15	2.95	0.028	0.085
65	Lamprophyre, Spanish Peaks, Colo.	2.872	2.860	2.874	2.855	2.879	0.07	0.66	0.00	*101.69	0.211	0.002

Sample Number	Rock Type & Locality	DBD	DBA	SGG	SGH	SGA	TOP	WAP	HAP	K x 10^3	k_d	$\Delta E/\Delta P$
				Mg/m^3			$100\left[1-\frac{DBD}{SGG}\right]$	$100\left[1-\frac{DBA}{SGA}\right]$	$100\left[1-\frac{DBD}{SGH}\right]$	S.I. units	μdarcies	mV/kP_a
66	Pyroxenite (Harzburgite), Stillwater Complex, Mont.	3.254	3.257	3.298	3.257	3.266	1.33	0.28	0.09	*0.99	2.19	0.054
67	Dunite (Olivine peridotite), Balsam, N. C.	3.139	3.153	3.173	3.161	3.172	1.07	0.60	0.70	*0.84	0.955	0.007
68	Pyroxenite-pigeonite, Louden, Co., Va.	2.950	2.965	2.979	2.966	2.983	0.97	0.60	0.54	46.97	0.377	0.041
69	Peridotite, Larimer Co., Colo.	2.558	2.549	2.709	2.690	2.702	5.57	5.66	4.91	0.69	44.0	0.007
70	Scoria, Mono County, Calif.	0.445	[3]0.833	2.359	1.934	1.889	81.14	55.90	76.99	0.13	$27.4x10^6$	0.893
71	Leucite nepheline tephrite, Laacher See, Germany	2.170	[3]2.267	2.857	2.844	2.862	24.05	20.79	23.70	*13.65	$0.011x10^6$	0.190
72	Amygdaloidal basalt, Grant Co., Oreg.	2.706	2.709	2.828	2.797	2.787	4.31	2.80	3.25	*24.55	0.047	<0.001
73	Basaltic obsidian, Sandoval Co., N. Y.	[1]2.265	2.324	2.421	2.402	2.383	6.44	2.48	5.70	5.26	1240.0	0.709

Sample Number	Rock Type & Locality	DBD	DBA	SGG	SGH	SGA	TOP	WAP	HAP	K x 10^3	k_d	$\Delta E/\Delta P$
				Mg/m^3			$100\left[1-\frac{DBD}{SGG}\right]$	$100\left[1-\frac{DBA}{SGA}\right]$	$100\left[1-\frac{DBD}{SGH}\right]$	S.I. units	μdarcies	mV/kP_a
74	Welded tuff, Inyo Co., Calif.	2.014	2.033	2.405	2.382	2.380	16.26	14.58	15.45	*3.22	958.4	0.116
75	Lapilli Tuff, Los Angeles Co., Calif.	2.092	2.108	2.684	2.679	2.691	22.06	21.66	22.26	4.25	1.37	<0.001
76	Tuff, Bishop, Calif.	[1]1.460	1.555	2.526	2.521	2.505	42.20	37.92	42.09	2.07	634.0	0.037
77	Kimberlite, Murfreesboro, Ark.	1.547	--	2.611	2.518	--	40.75	--	38.56	0.34	9.03	0.001
78	Sepentinite, Cardiff, Md.	2.641	2.638	2.667	2.646	2.661	0.97	0.86	0.19	118.93	0.651	0.003
79	Quartz pebble conglomerate, Nanticoke, Pa.	[1]2.432	2.522	2.675	2.670	2.628	9.08	4.03	8.91	0.01	133.0	0.257
80	Conglomerate, San Bernadino Co., Calif.	2.533	2.551	2.720	2.731	2.708	6.88	5.80	7.25	0.12	4.25	0.001
81	Jasper conglomerate, Buffalo Gap., S. Dak.	2.539	[3]2.580	2.669	2.649	2.649	4.87	2.60	4.15	0.03	0.100	0.024
82	Volcanic breccia, Guffey, Colo.	2.176	2.194	2.698	2.695	2.671	19.35	17.86	19.26	21.41	1.59	0.006
83	Gray sandstone, Berea, Ohio	2.129	[3]2.165	2.686	2.702	2.656	20.74	18.49	21.21	0.07	0.013×10^6	0.111

Sample Number	Rock Type & Locality	DBD	DBA	SGG	SGH	SGA	TOP	WAP	HAP	K x 10^3	k_d	$\Delta E/\Delta P$
				Mg/m^3			$100\left[1-\frac{DBD}{SGG}\right]$	$100\left[1-\frac{DBA}{SGA}\right]$	$100\left[1-\frac{DBD}{SGH}\right]$	S.I. units	μdarcies	mV/kP_a
84	Red sandstone, Potsdam, N.Y.	2.492	2.510	2.652	2.647	2.652	6.03	5.35	5.86	*0.06	4.15	0.171
85	Argillaceous sandstone, Portageville, N.Y.	2.493	2.490	2.701	2.721	2.718	7.70	8.39	8.38	0.25	0.915	0.011
86	Micaceous sandstone, Portland, Conn.	2.140	2.171	2.669	2.708	2.666	19.82	18.57	20.97	0.07	0.055×10^6	0.167
87	Brown sandstone, Medena, N.Y.	2.501	2.496	2.676	2.658	2.671	6.54	6.55	5.91	0.11	2.05	0.003
88	Banded sandstone, Buffalo, Gap., S. D.	2.055	--	2.685	2.679	--	23.46	--	23.29	0.04	--	--
89	Sandstone, Santa Clara Co., Calif.	2.160	[3]2.230	2.698	2.695	2.680	19.94	16.79	19.85	*0.50	926.0	0.010
90	Coconino sandstone, Mojave Co., Ariz.	2.383	2.401	2.677	2.672	2.649	10.98	9.29	10.82	0.04	26.2	0.006
91	Siltstone, Tick Canyon, Calif.	2.119	2.128	2.694	2.688	2.693	21.34	20.98	21.17	0.22	4.55	0.007
92	Arkose, Mt. Tom, Mass.	2.700	2.702	2.750	2.744	2.736	1.82	1.24	1.60	0.38	0.707	0.003
93	Graywacke, Grafton, N. Y.	2.703	2.705	2.737	2.732	2.732	1.24	0.99	1.06	0.32	N/M	0.006

Sample Number	Rock Type & Locality	DBD	DBA	SGG	SGH	SGA	TOP	WAP	HAP	$K \times 10^3$	k_d	$\Delta E/\Delta P$
		Mg/m^3					$100\left[1-\frac{DBD}{SGG}\right]$	$100\left[1-\frac{DBA}{SGA}\right]$	$100\left[1-\frac{DBD}{SGH}\right]$	S.I. units	μ darcies	mV/kP_a
94	Graywacke, Mentone, Calif.	2.551	2.589	2.708	2.711	2.714	5.80	4.61	5.90	6.69	4.49	0.006
95	Arenaceous shale, Ravena, N. Y.	2.691	2.710	2.736	2.717	2.724	1.64	0.51	0.96	0.18	0.233	0.003
96	Oil Shale, Garfield, Co., Colo.	2.113	2.105	2.235	2.163	2.132	5.46	1.27	2.31	0.10	2.54	0.010
97	Bauxite, Bauxite, Ark.	2.389	2.405	2.924	2.921	2.848	18.30	15.55	18.21	0.53	0.074	0.007
98	Chert, Joplin, Mo.	2.585	2.619	2.655	2.622	2.625	2.64	0.23	1.41	0.01	0.368	0.012
99	Novacalite, Hot Springs, Ark.	[1]2.578	2.642	2.661	2.660	2.652	3.12	0.38	3.08	<0.01	N/M	0.056
100	Flint, Dover, England	2.570	2.582	2.623	2.597	2.600	2.02	0.58	1.04	0.01	0.026	0.009
101	Siliceous oolite, State College, Pa.	2.273	2.275	2.661	2.647	2.633	14.58	13.60	14.13	0.01	258.0	0.061
102	Encrinal limestone, Lockport, N. Y.	2.683	2.673	2.763	2.730	2.729	2.90	2.05	1.72	0.04	0.504	0.006
103	Limestone, Garden Park, Colo.	2.673	2.663	2.724	2.702	2.690	1.87	1.00	0.63	*0.10	0.310	0.118
104	Chalk, Oktibbeha Co., Miss.	1.772	--	2.671	2.667	--	33.66	--	33.56	0.06	1.53	0.006

Sample Number	Rock Type & Locality	DBD	DBA	SGG	SGH	SGA	TOP	WAP	HAP	K x 10^3	k_d	$\Delta E/\Delta P$
		Mg/m^3					$100\left[1-\frac{DBD}{SGG}\right]$	$100\left[1-\frac{DBA}{SGA}\right]$	$100\left[1-\frac{DBD}{SGH}\right]$	S.I. units	μ darcies	mV/kP_a
105	Calcareous Tufa, Mumford, N. Y.	1.072	--	2.659	2.655	--	59.68	--	59.62	0.02	37.9×10^6	0.554
106	Common gray limestone, Mumford, N. Y.	2.580	2.583	2.845	2.832	2.782	9.31	7.15	8.90	0.12	3.31	0.033
107	Lithographic limestone, Solenhofen, Bavaria	2.607	2.607	2.717	2.709	2.706	4.05	3.66	3.77	0.03	0.682	0.004
108	Coquina, St. Augustina, Fla.	1.590	[3]2.196	2.732	2.730	2.679	41.80	18.03	41.76	*0.02	9.05×10^6	1.33
109	Limestone, Kasota, Minn.	2.543	2.569	2.846	2.840	2.812	10.65	8.64	10.46	0.06	15.1	0.019
110	Travertine, Tivoli, Italy	2.511	2.543	2.752	2.670	2.649	8.76	4.00	5.96	*0.17	0.317	0.030
111	Dolomitic limestone, Rochester, N. Y.	2.753	2.770	2.867	2.866	2.850	3.98	2.81	3.94	*0.25	3.97	0.088
112	Phosphorite, Conda, Idaho	2.659	--	3.086	3.063	--	13.84	--	13.19	0.03	73.6	0.044
113	Diffusion dolomite, Fremont, Colo.	2.531	2.563	2.848	2.836	2.845	11.13	9.91	10.75	0.05	16.1	0.016
114	Limestone, Bedford, Ind.	2.209	2.238	2.717	2.716	2.699	18.70	17.08	18.67	0.04	0.002×10^6	-0.035
115	Siliceous dolomite, Middleville, N.Y.	2.625	2.655	2.818	2.824	2.814	6.85	5.65	7.05	0.07	1.91	0.051

Sample Number	Rock Type & Locality	DBD	DBA	SGG	SGH	SGA	TOP	WAP	HAP	K x 10^3	k_d	$\Delta E/\Delta P$
				Mg/m^3			$100\left[1-\frac{DBD}{SGG}\right]$	$100\left[1-\frac{DBA}{SGA}\right]$	$100\left[1-\frac{DBD}{SGH}\right]$	S.I. units	μdarcies	mV/kP_a
116	Kona Dolomite, Stalwart, Mich.	2.841	2.844	2.876	2.861	2.848	1.22	0.14	0.70	0.05	0.283	0.006
117	Hematite limestone, Ontario, N. Y.	2.886	2.894	3.171	3.103	3.048	8.99	5.05	6.99	0.56	0.320	0.018
118	Siderite rock, Athens Mine, Anticline, Mich.	3.296	3.295	3.350	3.348	3.311	1.61	0.48	1.55	*21.09	0.640	0.002
119	Banded sandstone, Mansfield, Ohio	1.749	--	2.726	2.683	--	35.84	--	34.81	0.06	$2.00x10^6$	0.089
120	Ulexite, Boron, Calif.	[2]1.932	--	1.993	1.957	--	3.06	--	1.28	0.01	--	--
121	Gypsum, Washington Co., Utah	2.123	--	2.310	2.312	--	8.10	--	8.17	0.01	--	--
122	Rock gypsum, Grand Rapids, Mich.	2.235	--	2.372	2.340	--	5.78	--	4.49	0.01	--	--
123	Rock anhydrite, Hauts County, Nova Scotia	2.936	--	2.958	2.950	--	0.74	--	0.47	0.21	281.0	0.055
124	Anhydrite, Balmat, N. Y.	2.870	--	2.938	2.933	--	2.31	--	2.15	0.01	0.509	0.005
125	Trona, Westvaco, Wyo.	2.068	--	2.280	2.125	--	9.30	--	2.68	0.03	--	--
126	Cordierite hornfels, Helena, Mont.	2.711	2.709	2.735	2.719	2.717	0.88	0.29	0.29	14.40	1.47	0.003

Sample Number	Rock Type & Locality	DBD	DBA	SGG	SGH	SGA	TOP	WAP	HAP	K x 10^3	k_d	$\Delta E/\Delta P$
		Mg/m^3					$100\left[1-\frac{DBD}{SGG}\right]$	$100\left[1-\frac{DBA}{SGA}\right]$	$100\left[1-\frac{DBD}{SGH}\right]$	S.I. units	μdarcies	mV/kP_a
127	Hornfels, Riverside Co., Calif.	2.669	2.688	2.704	2.680	2.690	1.29	0.07	0.41	--	0.064	0.009
128	Pink marble, Tate, Ga.	2.716	2.724	2.737	2.736	2.726	0.77	0.07	0.73	0.08	1.24	0.234
129	Dolomite marble, Thornwood, N.Y.	2.844	2.836	2.885	2.875	2.856	1.42	0.70	1.08	0.04	4.96	-0.175
130	Verde Antique, Rochester, Vt.	2.657	2.648	2.704	2.670	2.662	1.74	0.53	0.49	*37.57	0.177	0.005
131	Graphitic marble, Crown Point, N. Y.	[1]2.611	2.746	2.767	2.762	2.755	5.64	0.33	5.47	0.03	3.05	0.040
132	Dolomite marble, Lucerne Valley, Calif.	2.782	2.822	2.841	2.831	2.825	2.08	0.11	1.73	0.09	0.146	0.028
133	Marble, San Bernadino, Co., Calif.	2.989	2.991	3.002	3.000	3.001	0.43	0.33	0.37	*0.21	0.135	-0.004
134	White marble, Rutland, Vermont	2.688	2.695	2.726	2.724	2.709	1.39	0.52	1.32	*0.04	13.2	0.104
135	Chocolate marble, Knoxville, Tenn.	2.683	2.698	2.722	2.700	2.706	1.43	0.30	0.63	0.04	1.04	0.003
136	Black marble, Isle La Motte, Vt.	2.689	2.702	2.727	2.725	2.711	1.58	0.33	1.50	*0.21	0.075	0.002
137	Marble, Goveneur, N. Y.	2.743	2.755	2.763	2.761	2.758	0.72	0.11	0.65	*0.21	0.555	0.082

Sample Number	Rock Type & Locality	DBD	DBA	SGG	SGH	SGA	TOP	WAP	HAP	K x 10^3	k_d	$\Delta E/\Delta P$
				Mg/m^3			$100\left[1-\frac{DBD}{SGG}\right]$	$100\left[1-\frac{DBA}{SGA}\right]$	$100\left[1-\frac{DBD}{SGH}\right]$	S.I. units	μdarcies	mV/kP_a
138	Limestone skarn, L. A. Co., Calif.	3.002	3.012	3.187	3.144	3.089	5.80	2.49	4.52	0.24	104.0	0.177
139	Garnet-idocrase rock, Xalostoc, Mexico	2.808	2.826	3.042	2.985	2.988	7.69	5.42	5.93	*0.30	0.811	0.519
140	Quartzite, Ableman, Wis.	2.651	2.645	2.669	2.658	2.648	0.67	0.11	0.26	0.02	0.026	0.046
141	Quartzite, Ishpeming, Mich.	2.666	2.683	2.717	2.701	2.691	1.88	0.30	1.30	1.40	0.679	0.034
142	Quartzite, Melrose, Mont.	2.728	2.733	2.750	2.745	2.743	0.80	0.36	0.62	0.06	0.291	0.045
143	Chlorite Schist, Chester, Vt.	2.921	2.926	3.033	2.930	2.946	3.69	0.68	0.31	*4.15	0.070	0.025
144	Stilpnomelane Schist, Longvale Quarry, Calif.	3.018	3.045	3.135	3.131	3.155	3.73	3.49	3.61	1.39	1.78	0.028
145	Andalusite slate, Mariposa Co., Calif.	2.773	2.763	2.791	2.790	2.771	0.64	0.29	0.61	0.66	3.58	0.003
146	Red Slate, Granville, N.Y.	[1]2.673	2.762	2.791	2.752	2.774	4.23	0.43	2.87	0.21	0.078	0.004
147	Chiastolite slate, San Gabriel, Calif.	2.752	2.767	2.791	2.769	2.774	1.40	0.25	0.61	0.40	0.761	0.009
148	Green slate, Pawlet, Vt.	2.759	2.790	2.819	2.818	2.802	2.13	0.43	2.09	0.43	0.079	0.002

Sample Number	Rock Type & Locality	DBD	DBA	SGG	SGH	SGA	TOP	WAP	HAP	K x 10^3	k_d	$\Delta E/\Delta P$
				Mg/m^3			$100\left[1-\frac{DBD}{SGG}\right]$	$100\left[1-\frac{DBA}{SGA}\right]$	$100\left[1-\frac{DBD}{SGH}\right]$	S.I. units	μ darcies	mV/kP_a
149	Staurolite quartzite, Big Rock, Mexico	2.965	2.970	3.049	3.032	3.034	2.76	2.04	2.21	6.77	1.19	0.203
150	Kyanite quartzite, Ogilby, Calif.	3.037	3.033	3.076	3.074	3.058	1.27	0.82	1.20	0.05	4.18	0.008
151	Sillimanite-garnet, gneiss, Hague, N. Y.	3.130	3.137	3.157	3.155	3.144	0.86	0.22	0.79	0.94	0.916	0.005
152	Cordierite-anthophyllite skarn, Betty Mine, Colo.	3.036	3.044	3.067	3.065	3.059	1.01	0.49	0.95	1.07	0.687	0.006
153	Augen gneiss, Grass Lake, N.Y.	2.638	2.645	2.695	2.651	2.661	2.12	0.60	0.49	10.04	0.650	0.040
154	Granitoid gneiss, Salisbury, N. C.	2.598	2.617	2.667	2.622	2.633	2.59	1.73	0.92	10.06	0.622	0.175
155	Biotite gneiss, Uxbridge, Mass.	2.699	2.724	2.759	2.739	2.747	3.26	0.84	2.56	0.31	6.59	0.227
156	Hornblende gneiss, Clintonville, N.Y.	3.006	3.042	3.090	3.043	3.055	2.72	0.43	1.22	0.71	0.184	0.011
157	Augen gneiss, San Bernadino Co., Calif.	2.705	2.711	2.753	2.752	2.748	1.74	1.35	1.71	20.18	4.91	0.163
158	Diorite gneiss, San Bernadino Co., Calif.	2.703	2.704	2.750	2.748	2.733	1.71	1.06	1.64	8.73	6.23	0.084

Sample Number	Rock Type & Locality	DBD	DBA	SGG	SGH	SGA	TOP	WAP	HAP	K x 10^3	k_d	$\Delta E/\Delta P$
				Mg/m^3			$100\left[1-\frac{DBD}{SGG}\right]$	$100\left[1-\frac{DBA}{SGA}\right]$	$100\left[1-\frac{DBD}{SGH}\right]$	S.I. units	μ darcies	mV/kP_a
159	Eclogite, Healdsburg, Calif.	3.230	3.251	3.259	3.248	3.254	0.89	0.09	0.55	0.94	0.013	0.013
160	Eclogite, Almenningen, Norway	[1]3.300	3.359	3.416	3.407	3.371	3.40	0.36	3.14	0.31	0.935	0.009
161	Cummingtonite Schist, Rockford, S. Dak.	3.393	3.403	3.575	3.428	3.423	5.09	0.58	1.02	*12.77	0.539	0.005
162	Hornblende schist, Mitchell Co., N. C.	3.086	3.097	3.147	3.100	3.106	1.94	0.29	0.45	*0.69	0.329	0.012
163	Glaucophane schist, Sonoma Co., Calif.	3.073	3.076	3.249	3.192	3.168	5.42	2.90	3.73	0.85	N/M	0.045
164	Albite-muscovite schist, San Bernadino Co., Calif.	2.763	2.777	2.809	2.793	2.800	1.64	0.82	1.07	0.25	0.341	0.049
165	Phyllite, Woodbridge, Conn.	[1]2.615	2.745	2.798	2.780	2.777	6.54	1.15	5.94	0.36	0.200	0.008
166	Stilpnomelane schist, Otago, New Zealand	[1]2.782	2.880	2.957	2.925	2.938	5.92	1.97	4.89	0.71	6.34	0.097
167	Vishnu schist, Ariz.	2.630	2.638	2.679	2.665	2.668	1.83	1.12	1.31	0.11	0.294	0.005
168	Mica schist, Manhattan, N. Y.	2.652	--	2.805	2.759	--	5.45	--	3.88	*0.37	0.275	0.010

Sample Number	Rock Type & Locality	DBD	DBA	SGG	SGH	SGA	TOP	WAP	HAP	K x 10^3	k_d	$\Delta E/\Delta P$
		Mg/m^3					$100\left[1-\frac{DBD}{SGG}\right]$	$100\left[1-\frac{DBA}{SGA}\right]$	$100\left[1-\frac{DBD}{SGH}\right]$	S.I. units	μ darcies	mV/kP_a
169	Talc-tremolite schist, St. Lawrence Co., N. Y.	2.634	--	2.801	2.771	--	5.96	--	4.94	0.02	0.063	0.058
170	Slate, Bangor, Pa.	2.678	--	2.815	2.783	--	4.87	--	3.77	*0.43	0.085	0.005
171	Quartz sericite schist, Montgomery Co., Ps.	2.640	--	2.728	2.687	--	3.23	--	1.75	0.13	42.8	0.386
172	Chlorite schist, Calavaras Co., Calif.	2.704	2.707	2.737	2.727	2.729	1.21	0.81	0.84	*0.58	0.241	0.004
173	Epidosite, Lookout Mtn., Colo.	3.097	3.126	3.188	3.186	3.164	2.85	1.20	2.79	12.23	0.090	0.004
174	Jaspilite, Negaunee, Mich.	3.199	3.229	3.541	3.271	3.252	9.86	0.71	2.20	5.28	N/M	0.032
175	Grunerite magnetite rock, Michigamme, Mich.	3.829	3.824	3.884	3.881	3.875	1.42	1.32	1.34	1844.74	0.312	0.002
176	Hexagonite, Fowler, N. Y.	[1]2.588	2.631	2.746	2.743	2.736	5.75	3.84	5.65	0.08	0.115	<0.001
177	Piemontite mica, L. A. Co., Calif.	2.667	2.669	2.713	2.681	2.694	1.70	0.93	0.52	0.10	1.05	0.039
178	Actinolite, Chester, Vt.	[1]2.936	3.027	3.078	3.076	3.043	4.61	0.53	4.55	*0.68	0.591	0.006

Sample Number	Rock Type & Locality	DBD	DBA	SGG	SGH	SGA	TOP	WAP	HAP	K x 10^3	k_d	$\Delta E/\Delta P$
				Mg/m^3			$100\left[1-\frac{DBD}{SGG}\right]$	$100\left[1-\frac{DBA}{SGA}\right]$	$100\left[1-\frac{DBD}{SGH}\right]$	S.I. units	μ darcies	mV/kP_a
179	Unakite, Rockbridge, Co., Va.	2.938	2.938	2.983	2.964	2.979	1.51	1.38	0.88	0.59	1.41	0.019
180	Greenstone, Ely, Minn.	2.989	3.005	3.005	2.996	3.008	0.53	0.10	0.23	1.34	0.023	0.025
181	Emery, Peckskill, N. Y.	3.311	3.313	3.317	3.316	3.316	0.18	0.09	0.15	99.27	0.675	0.002
182	Red ochre, Keystone, S. Dak.	2.588	2.617	3.609	3.600	3.622	28.29	27.75	28.11	1.04	880.0	0.005

[1] Samples are chipped on edges
[2] Sample partially dissolved during saturation
[3] Vuggy and/or very porous samples

Table 2--Average densities and porosities of 165 samples from Table 1 classified according to major rock systems. Some samples from table 1 were excluded because there were no SGA or DBA measurements made.

ROCK GROUP	DBD	DBA	SGG	SGH	SGA	TOP	HAP	WAP	Fractional occluded porosity 1- (WAP/TOP)
			Mg/m^3				%		
IGNEOUS	2.525	2.544	2.751	2.703	2.701	5.91	5.16	4.64	0.22
SEDIMENTARY	2.488	2.524	2.748	2.737	2.719	9.50	9.06	7.20	0.24
METAMORPHIC	2.864	2.885	2.958	2.933	2.932	3.07	2.27	1.42	0.54

Table 3--Average permeabilities and electrokinetic coupling coefficients of selected rock types or groups. Rocks having permeabilities of greater than 10 μ darcies are not included because those values are anomalously high with respect to average permeabilities.

Rock type or Rock Group	Number of Samples	Permeability, k_d (μ darcies)	Electrokinetic coupling coefficient, $(\frac{\Delta E}{\Delta P})$ (mV/kPa)	$\Delta E/\Delta P/k_d$ (mV/kP$_a$/μ darcy)	Standard deviations k_d	Standard deviations $\Delta E/\Delta P$
Granite, Aplite, Trachyte, Phonolite	18	1.70	0.045	0.026	1.81	0.034
Quartz Monzonite, Monzonite Granodiorite, Latite	7	0.725	0.006	0.008	0.584	0.004
Dacite, Andesite, Diorite, Tonalite	7	0.338	0.008	0.024	0.543	0.010
Gabbro, Norite, Basalt, Diabase	11	1.26	0.025	0.020	3.061	0.026
Sandstone, Arkose, etc.	7	2.41	0.030	0.012	1.96	0.062
Limestone, Dolomite	10	1.31	0.036	0.027	1.36	0.039
Marble	9	0.960	0.064	0.067	1.56	0.085
Slate, Phyllite	6	0.797	0.005	0.006	1.39	0.003
Schist	10	1.03	0.029	0.028	1.93	0.030
Gneiss	7	2.87	0.101	0.035	2.90	0.088

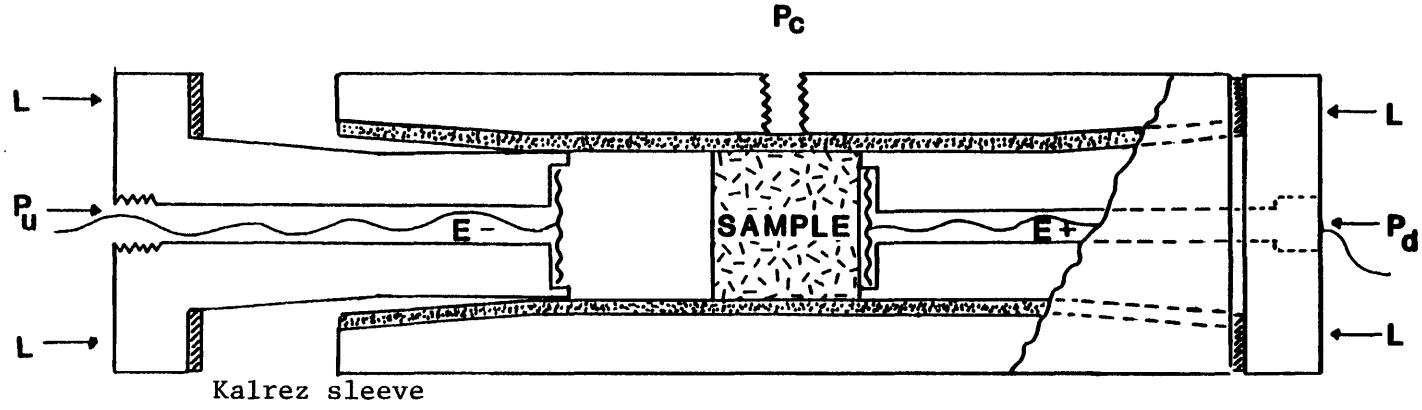

Figure 1. Stainless steel flow cell used to measure permeability and streaming potential. The sample is contained within a Kalrez sleeve and sealed with end pieces clamped by load, L. P_u and P_d are independently controlled pore pressures and P_c is confining pressure. Streaming potential is measured between platinum mesh electrodes E+ and E-. Insulated wires are brought to the outside via pressure feed throughs. Capillary tube is attached to P_d for permeability measurements.

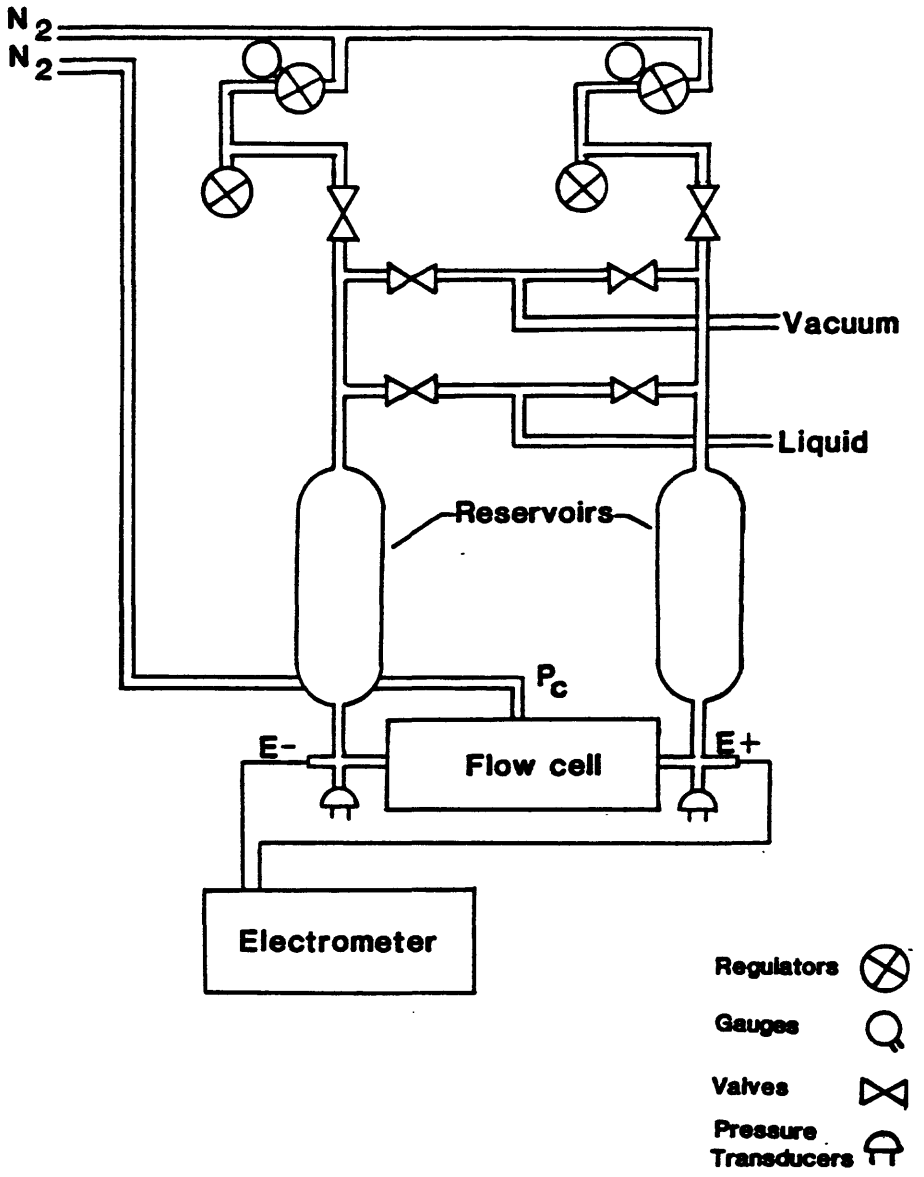

Figure 2. Diagram of streaming potential system. Components below uppermost valves are evacuated and partially backfilled with liquid. Confining pressure (P_c) and pore pressure (shown in Figure 1) are all independently controlled with nitrogen gas.

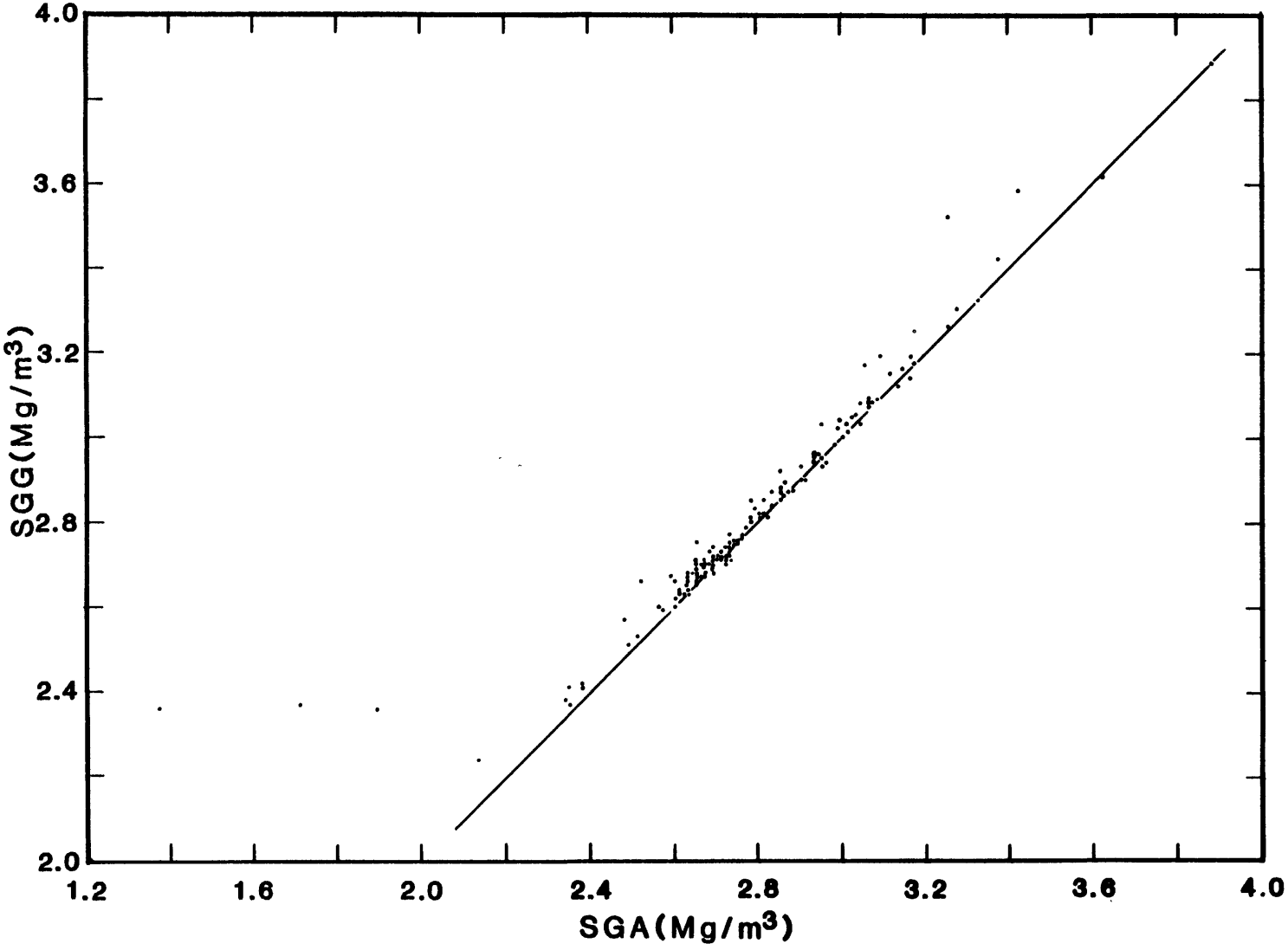

Figure 3. Relationship between grain densities using Archimedes' principle (SGA) and helium pycnometry of powdered samples (SGG). On the solid line SGA = SGG. The three points that deviate considerably from the line represent samples of pumice.

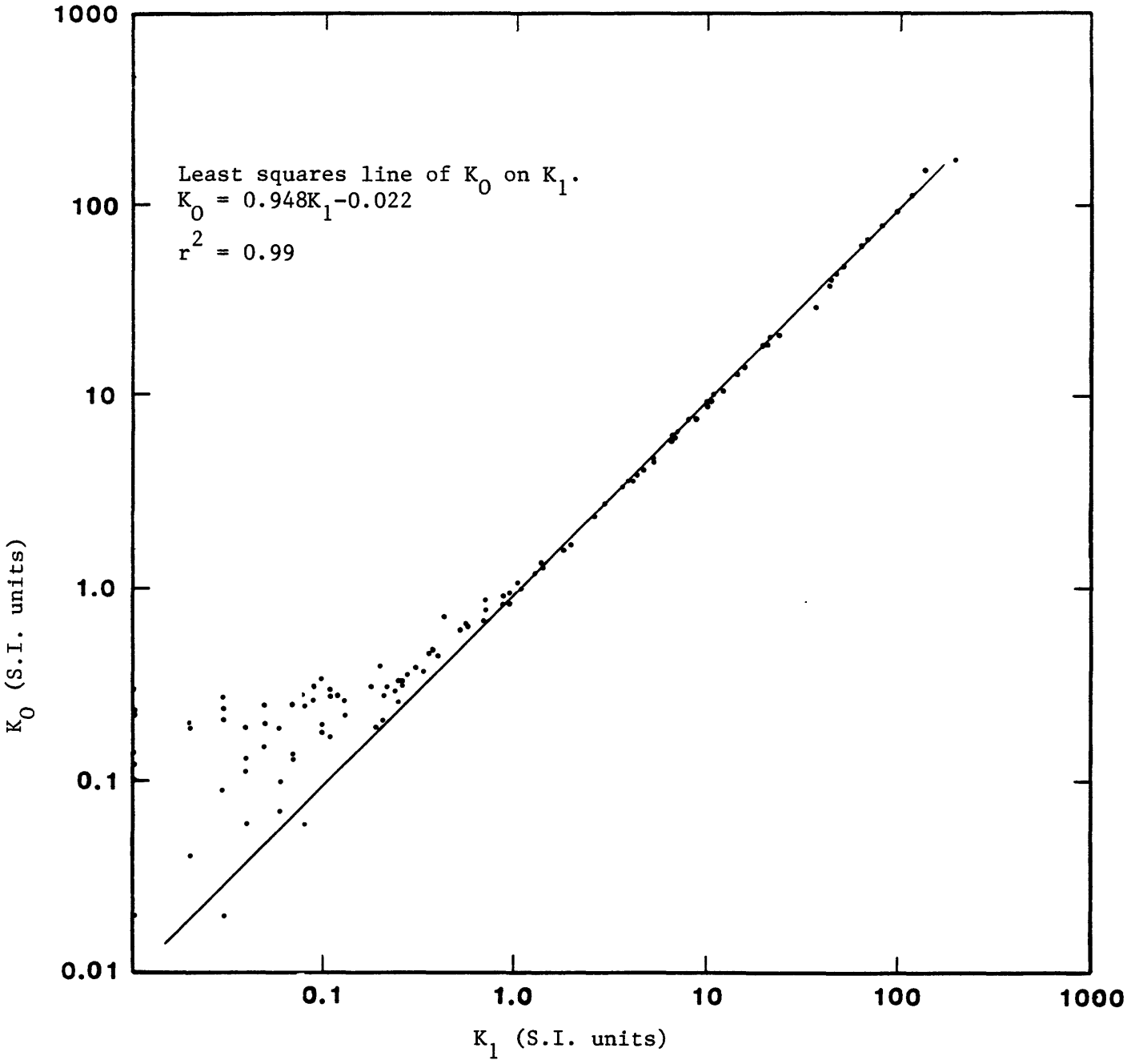

Figure 4. Relationship between magnetic susceptibility measurements made on Bison bridge (K_0) and U.S.G.S. instrument (K_1). r^2 is the coefficient of determination.

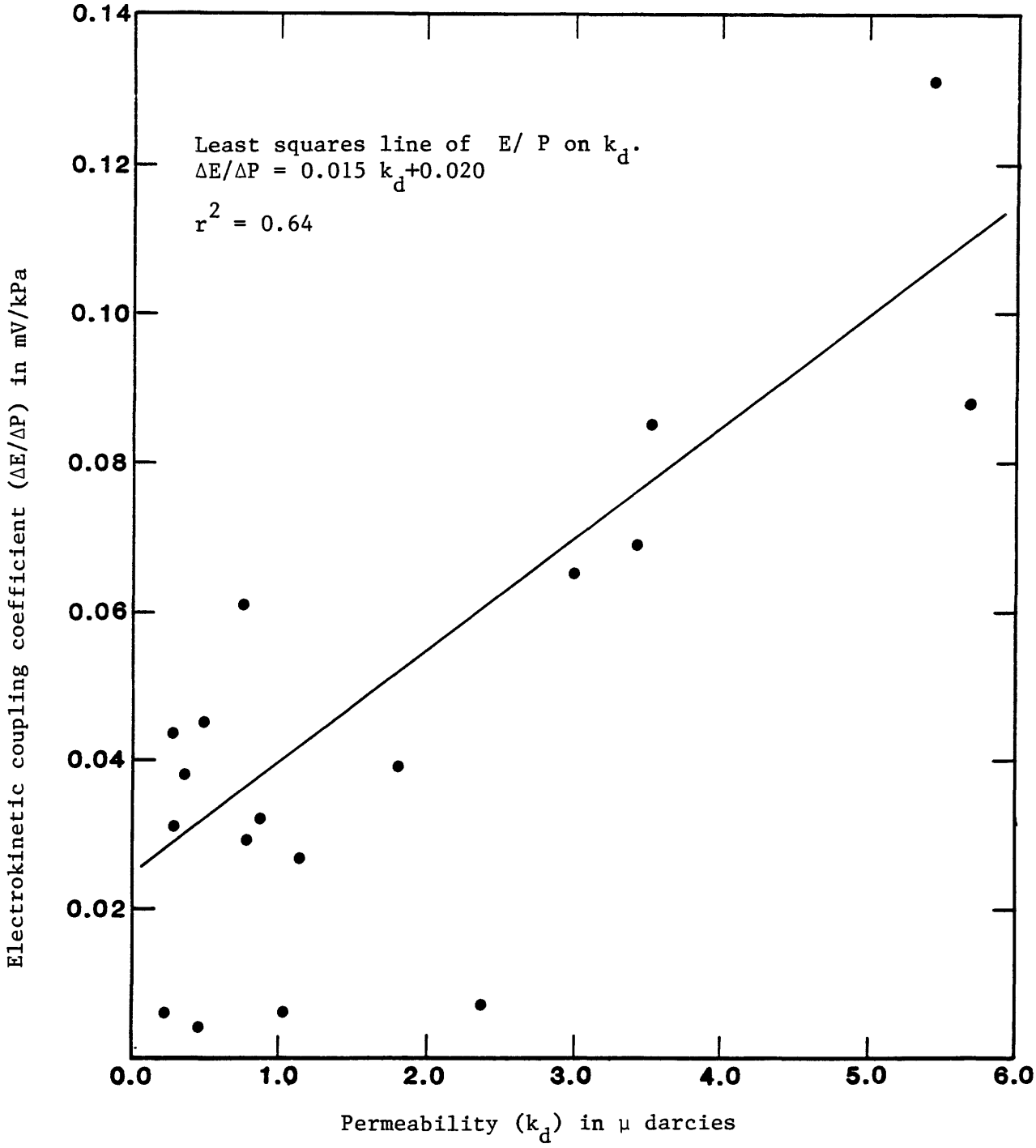

Figure 5. Relationship between permeability and electrokinetic coupling coefficient of granites and related rocks from Table 3.